Time-Dependent Anti-inflammatory Effects of a Lipid Extract from *Macrocystis pyrifera* on Toll-Like Receptor 2 Signaling in Human THP-1 Monocytes

Authors
Jamie Mei Lin Kok[1], Georgina Dowd[2], Jaydee Cabral[3], Lyn Wise[1]

Affiliations
1 Department of Pharmacology and Toxicology, School of Biomedical Sciences, University of Otago, Dunedin, New Zealand
2 The New Zealand Institute for Plant & Food Research Limited, Nelson, New Zealand
3 Department of Chemistry, University of Otago, Dunedin, New Zealand

Key words
Macrocystis pyrifera (Linnaeus) C. Agardh, Phaeophyta, Laminariaceae, fractionation, fatty acid, inflammation, Toll-like receptor, NFκB

received 19.09.2021
revised 13.12.2021
accepted 22.12.2021
published online 2022

Bibliography
Planta Med Int Open 2022; 9: e80–e89
DOI 10.1055/a-1729-3654
ISSN 2509-9264

Georg Thieme Verlag, Rüdigerstraße 14,
70469 Stuttgart, Germany

Correspondence
Dr. Lyn Wise
Department of Pharmacology and Toxicology
School of Biomedical Sciences
University of Otago
18 Frederick Street
9054 Dunedin
New Zealand
Tel.: + 64/3/479 7723, Fax: + 64/3/479 9140
lyn.wise@otago.ac.nz

Supporting information available online at http://www.thieme-connect.de/products.

ABSTRACT

Seaweeds reportedly contain anti-inflammatory compounds; however, little is known about the therapeutic potential of *Macrocystis pyrifera*. This study investigated the anti-inflammatory properties of a methanol:chloroform extract, chromatographic fractions, and fatty acids identified from *M. pyrifera* (Linnaeus) C. Agardh. In human THP-1 monocytes stimulated with the Toll-like receptor 2 agonist lipoteichoic acid, the extract decreased mRNA and protein levels of interleukin-1β, interleukin-8, and monocyte chemoattractant protein-1 to varied degrees at nontoxic concentrations. The greatest anti-inflammatory effects were elicited when the extract was applied between 6 h prior to, and 6 h after, the stimuli. Reduced levels of nuclear factor kappa-light-chain-enhancer of activated B cells signaling proteins were observed in extract-treated cells, with a significant decrease in the myeloid differentiation factor 88 protein abundance relative to stimulated THP-1 cells. Chromatographic fractionation of the extract yielded 40 fractions, of which fraction F25 exhibited the greatest inhibition of monocyte chemoattractant protein-1 production in activated THP-1 cells. Fatty acids abundant within the extract and F25 were identified then tested, individually and in combination, for their anti-inflammatory effects. Myristic acid, palmitoleic acid, and α-linolenic acid, but not the fatty acid combination, inhibited lipoteichoic acid-stimulated monocyte chemoattractant protein-1 production without compromising THP-1 cell viability. These findings indicate that the fatty acid-rich extract and fraction from *M. pyrifera* provide anti-inflammatory and cytoprotective effects that may be beneficial for use as a therapeutic.

ABBREVIATIONS

FAMEs	fatty acid methyl esters
GAPDH	glyceraldehyde-3-phosphate dehydrogenase
GC-MS	gas chromatography-mass spectrophotometry
HRP	horseradish peroxidase
Ig	immunoglobulin
IL	interleukin
LPS	lipopolysaccharide
LTA	lipoteichoic acid
MCP	monocyte chemoattractant protein
MYD88	myeloid differentiation primary response 88
NFκB	nuclear factor kappa-light-chain-enhancer of activated B cells
RP-HPLC	reversed-phase high-performance liquid chromatography
SD	standard deviation
TLR	Toll-like receptor
TNF	Tumor necrosis factor

Introduction

Macrocystis pyrifera, also known as giant kelp, is a large brown seaweed common along the eastern and southern coasts of the Pacific Ocean. This seaweed grows naturally in dense kelp forests, with wild harvest and aquaculture generating 1–200000 tons per annum, worldwide [1–3]. Commercial products obtained from *M. pyrifera* include animal and aquaculture feed, protein or dietary supplements, alginate dressings, and biofuels [3]. But seaweeds, such as giant kelp, are also recognized as a valuable source of natural products, with investigations increasing into medicinal uses for their bioactive compounds [4].

Inflammation initiates immune responses, which restore tissue homeostasis after damage or infection occurs. However, excessive inflammation leads to chronic conditions from autoimmune, cardiovascular, and neurodegenerative diseases to gastrointestinal, liver, lung, kidney, joint, and skin disorders [5]. Inflammation is initiated through TLRs, which are abundant on innate immune cells [6]. TLRs recognize pathogen- or damage-associated molecular patterns, such as LTA from gram-positive bacteria and LPS from gram-negative bacteria [7, 8]. TLR4 senses LPS from mucosal commensals and pathogens within the upper respiratory and gastrointestinal tracts and has a pathogenic role in severe sepsis and shock [9]. TLR2 reacts strongly to LTA derived from commensals such as *Staphylococcus aureus,* which is predominantly found in the anterior nares, but causes a variety of diseases from simple skin infections to sepsis and pneumonia [10]. Stimulation of either TLR2 or TLR4 leads to recruitment of adaptor proteins, including MYD88, which trigger signaling pathways that activate NFκB [11]. NFκB controls the transcription of proinflammatory cytokines [i. e., IL-1β and TNF-α] and chemokines [i. e., MCP-1 and IL-8], which provide instructions to adaptive immune cells [12]. Steroidal and nonsteroidal anti-inflammatory drugs targeting these inflammatory signaling pathways are used clinically, but their frequent and adverse effects, including gastrointestinal complications [13], renal failure [14], and hypersensitivity reactions [15], result in high rates of morbidity. As a result, there is growing interest in anti-inflammatory compounds from natural sources.

Anti-inflammatory activity has been observed for extracts and compounds derived from a range of seaweed varietals. Many studies have demonstrated that seaweed extracts inhibit inflammation induced by LPS via TLR4, but little is known regarding their effects on LTA- and TLR2-mediated inflammation. In LPS-activated human macrophages, a lipid extract from *Palmaria palmata* was found to decrease the synthesis of IL-6 and IL-8 [16]. TNF-α, IL-1β, and IL-6 production in LPS-stimulated murine macrophages was also inhibited by an ethanolic preparation of the brown algae *Ishige okamurae* [17]. Brown algae carotenoids from *Myagropsis myagroides, Sargassum siliquastrum*, and *I. okamurae* reduced the generation of nitric oxide and proinflammatory cytokines in LPS-treated murine macrophages and protected fibroblasts from oxidative stress-induced mortality [18–20]. By contrast, the sulphated polysaccharide fucoidan isolated from *M. pyrifera* activated immune cells, including natural killer cells, dendritic cells, and T cells [21]. While the biochemical makeup and the immunomodulatory activities of *M. pyrifera* fucoidan have been reported [21, 22], there has been little investigation on the anti-inflammatory activity of other constituents. The purpose of this study was therefore to prepare and characterize a lipid extract from *M. pyrifera*, then investigate its anti-inflammatory effects on TLR2-induced inflammatory signaling in human monocytes to provide insight into its utility as an anti-inflammatory therapy specifically for staphylococcal diseases.

Results

Methanol:chloroform (2:1) extraction from dried *M. pyrifera* blades yielded 1.50 % of total dry weight. Metabolic analysis was performed to assess cytotoxicity of the extract for human THP-1 monocytes. Ethanol was utilized as a positive control due to its known cytotoxic effects for human cell lines [23]. At extract concentrations greater than 0.25 mg.mL^{-1}, cells showed reduced viability relative to the vehicle only control ($p \leq 0.05$) (**Fig. 1Sa**, Supporting Information). At ethanol concentrations greater than 5 % (v/v), cells demonstrated decreased viability ($p \leq 0.05$) (**Fig. 1Sb**, Supporting Information). For subsequent experiments, a nontoxic concentration of extract (0.13 mg.mL^{-1}) dissolved in 1 % (v/v) ethanol was used.

THP-1 cells were stimulated with TLR2 agonist LTA and treated with *M. pyrifera* extract, with effects on proinflammatory cytokine production determined using ELISA. IL-10 was used as a positive control due to its anti-inflammatory effects on innate and adaptive immune cells [24]. In response to stimulation, THP-1 cells showed increases in MCP-1, IL-8, and IL-1β production (▶ **Fig. 1**). MCP-1 production was significantly reduced by 2, 6, and 24 h pretreatment, cotreatment, and 2 and 6 h posttreatment, with the greatest reduction following concurrent LTA and extract treatment (≈ 90 %, $p \leq 0.05$) (▶ **Fig. 1a**). LTA-stimulated IL-8 production also showed the greatest reduction with concurrent treatment (≈ 40 %, $p \leq 0.05$) (▶ **Fig. 1b**). IL-1β production in LTA-stimulated THP-1 cells was significantly reduced by 2 and 6 h pretreatment, cotreatment, and 2 and 6 h posttreatment, with the greatest reduction following concurrent LTA and extract treatment (≈ 80 %, $p \leq 0.05$) (▶ **Fig. 1c**).

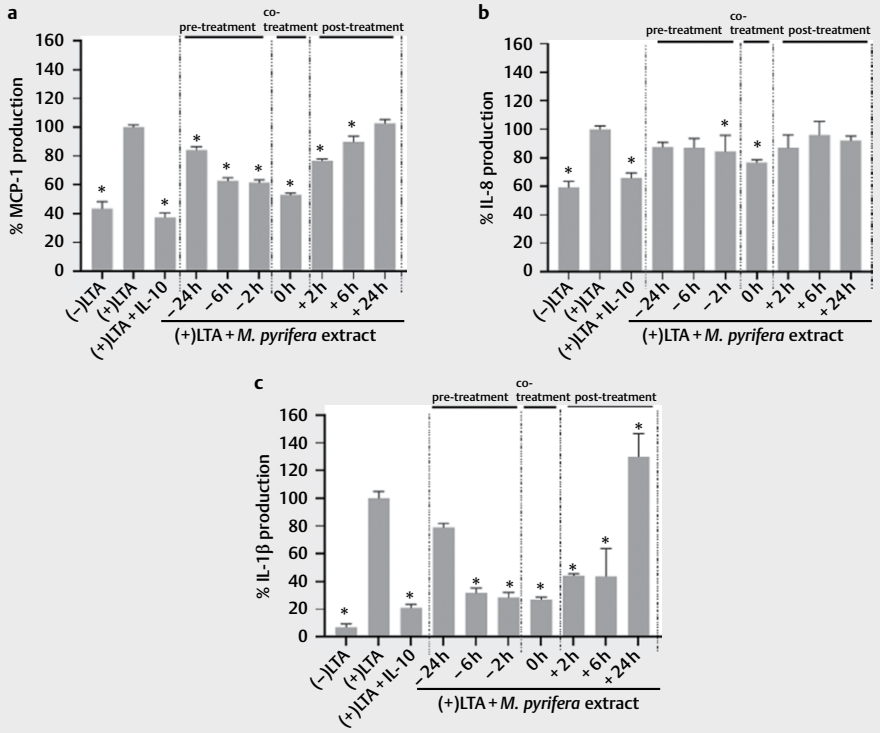

▶ **Fig. 1** Suppression of LTA-induced proinflammatory cytokine production in THP-1 cells by *M. pyrifera* extract. THP-1 cells were stimulated by LTA (1 µg.mL^{-1}), with or without pre-, co-, or post-treatment with extract (0.13 mg.mL^{-1}) or cotreatment with IL-10 (10 ng.mL^{-1}). After 24 h incubation with the extract, the conditioned medium was collected and assayed for (**a**) MCP-1, (**b**) IL-8, and (**c**) IL-1β production by ELISA. (+)LTA represents THP-1 cells stimulated with LTA only. (-)LTA represents unstimulated THP-1 cells. Values are expressed as a percentage of the (+)LTA control and presented as the mean ± SD (n = 3), with those that differ significantly from the (+)LTA control identified by one-way ANOVA followed by a Dunnett's test ($^*p \le 0.05$).

However, increased IL-1β production was observed when the extract was applied 24 h after LTA stimulation (≈ 30 %, $p \le 0.05$). As this increase would be undesirable therapeutically, production of IL-1β was assessed after 48 h incubation. At this timepoint, the extract reduced IL-1β production relative to LTA-stimulated cells (≈ 77 %, $p \le 0.05$) (**Fig. 2S**, Supporting Information). IL-10 also significantly inhibited MCP-1, IL-8, and IL-1β production in LTA-activated THP-1 cells by 80–110 % ($p \le 0.05$) (▶ **Fig. 1a–c**).

To ascertain whether the inhibitory effects of the *M. pyrifera* extract were specific to TLR2-induced inflammation, the extract was also applied to THP-1 cells stimulated with the TLR4 agonist LPS. MCP-1 production in response to LPS stimulation was suppressed by ≈ 66 % by concurrent treatment with the extract ($p \le 0.05$) (**Fig. 3S**, Supporting Information). IL-10 also significantly inhibited MCP-1 production in LPS-activated THP-1 cells by 86 % ($p \le 0.05$) (**Fig. 3S**, Supporting Information).

To assess whether *M. pyrifera* extract impacts proinflammatory gene transcription in LTA-stimulated THP-1 cells, mRNA was extracted, and levels were assessed relative to a reference gene using quantitative PCR. As IL-1β mRNA levels increased 3 and 6 h after LTA stimulation (**Fig. 4S,** Supporting Information), transcriptional analyses were conducted 4 h poststimulation. In response to stimulation, cells showed increases in the mRNA expression of MCP-1, IL-8, and IL-1β (▶ **Fig. 2a–c**). Cotreatment with the extract showed significant reductions in MCP-1 (≈ 56 %), IL-8 (≈ 73 %), and IL-1β (≈ 100 %) levels ($p \le 0.05$) (▶ **Fig. 2a–c**) relative to the LTA-stimulated controls. MCP-1 expression was also reduced by 2 h posttreatment (≈ 47 %) but not 2 h pretreatment with the extract (**Fig. 5Sa**, Supporting Information). Expression of IL-8 and IL-1β was reduced by 2 h pretreatment (≈ 95 % and ≈ 99 %, respectively) and 2 h posttreatment (≈ 66 % and ≈ 100 %, respectively) with the extract (**Fig. 5Sb, c**, Supporting Information).

To determine how the *M. pyrifera* extract impacts TLR2 signaling in LTA-activated THP-1 cells, cell lysates were collected after 4 h incubation, and NFκB signaling was investigated using a proteome profiler. In response to LTA stimulation, cells showed increases in MYD88, NFκB2 (p100), and REL-A/p65 (pS529) protein levels, which were inhibited to below that of unstimulated controls by extract cotreatment (**Fig. 6S**, Supporting Information). Treatment with the extract alone resulted in MyD88 and NFκB2 levels below that of unstimulated cells (**Fig. 6S**, Supporting Information). To validate these observations, the abundance of MYD88 was determined using immunocytochemistry and Western blot analyses. MYD88 was observed as small speckles stained within the cytoplasm (▶ **Fig. 3a**) and 38–40 kDa bands in Western blots (▶ **Fig. 3c**). In response to LTA stimulation, cells showed a 2-fold increase in MYD88 staining intensity ($p \le 0.05$) (▶ **Fig. 3a, b**) and 1.3-fold increase in MYD88 band density (▶ **Fig. 3c, d**) relative to unstimulated controls. Cotreatment with the extract significantly reduced MyD88 staining

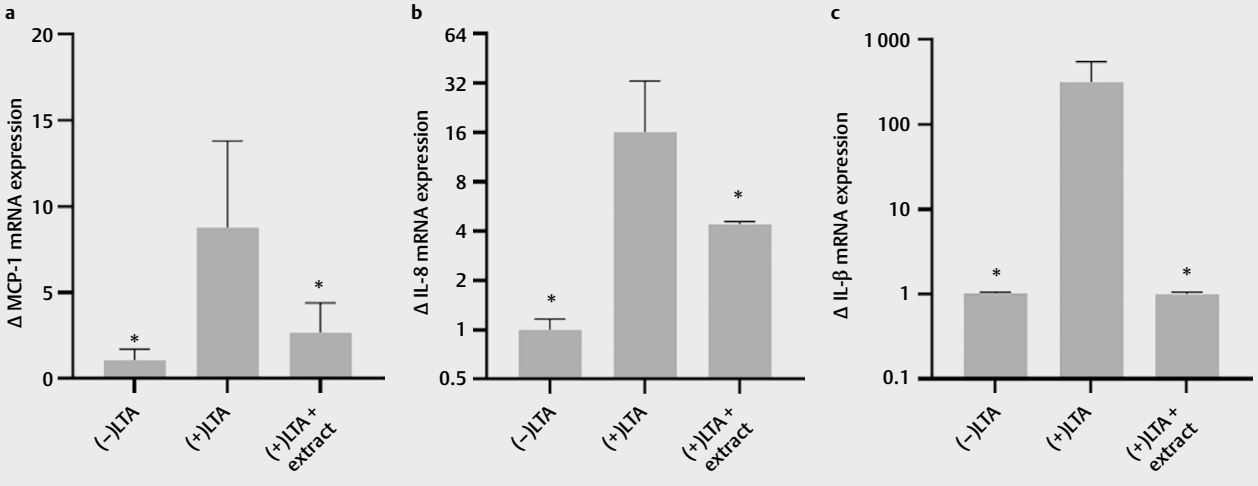

▶ **Fig. 2** Suppression of proinflammatory cytokine gene expression in stimulated THP-1 cells by *M. pyrifera* extract. (**a**–**c**) THP-1 cells were stimulated by LTA (1 µg.mL^{-1}) with or without cotreatment with the extract (0.13 mg.mL^{-1}). After 4 h incubation, RNA was isolated, reverse transcribed, and mRNA expression of (**a**) MCP-1, (**b**) IL-8, and (**c**) IL-1β was detected by quantitative PCR. Values are expressed relative to the (-)LTA control and reference gene, GAPDH, and are presented as the mean ± SD (n = 3), with those that differ significantly from the (+)LTA control identified by one-way ANOVA followed by a Dunnett's test ($^{*}p \leq 0.05$).

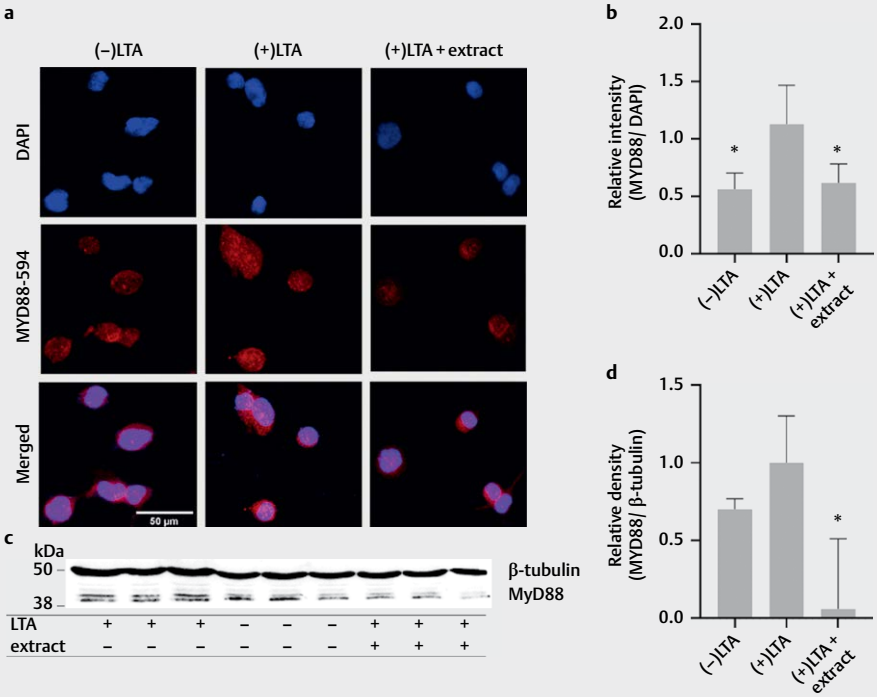

▶ **Fig. 3** Reduction in MYD88 levels in stimulated THP-1 cells following treatment with *M. pyrifera* extract. THP-1 cells were stimulated with LTA (1 µg.mL^{-1}) with or without cotreatment with the extract (0.13 mg.mL^{-1}) for 4 h. (**a**) Representative images of THP-1 cells stained using a rabbit anti-MYD88 polyclonal and goat anti-rabbit AlexaFluor-594 antibody (red), with nuclei stained using DAPI (blue). Scale bar, 50 µm. (**b**) MYD88 fluorescence intensity was calculated for each image. Values are expressed relative to the (+)LTA control and nuclear stain, DAPI, and presented as the mean ± SD (n = 5). (**c**) Representative image of Western blot analysis of THP-1 cell lysates following stimulation and/or treatment as indicated. (**d**) MYD88 band density was determined from each Western blot. Values are expressed relative to the (+)LTA control and loading control, β-tubulin, and presented as the mean ± SD (n = 3), with those that differ significantly from the (+)LTA control identified by one-way ANOVA followed by a Dunnett's test ($^{*}p \leq 0.05$).

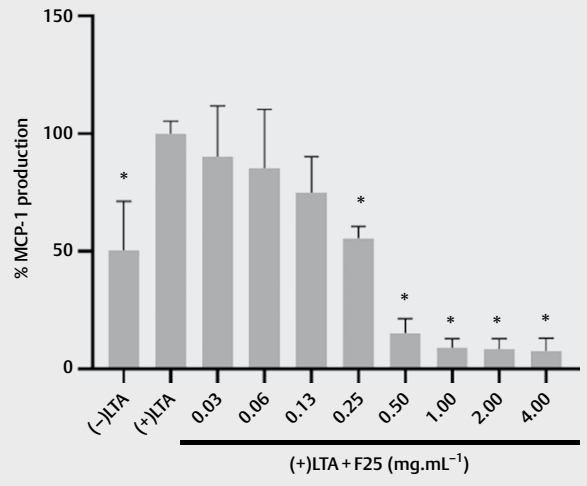

▶ **Fig. 4** Dose-dependent suppression of MCP-1 production in stimulated THP-1 cells by *M. pyrifera* fraction F25. THP-1 cells were stimulated by LTA (1 µg.mL^{-1}) with or without cotreatment with F25 (0.01–1.25 mg.mL^{-1}). After 24 h incubation, the conditioned medium was collected and assayed for MCP-1 production by ELISA. Values are expressed as percentage of the (+)LTA control and presented as the mean ± SD (n = 3), with those that differ significantly from (+)LTA control identified by one-way ANOVA followed by Dunnett's test (* $p \leq 0.05$).

intensity (≈ 45 %, $p \leq 0.05$) (▶ **Fig. 3b**) and band density (≈ 29.70 %, $p \leq 0.05$) (▶ **Fig. 3d**).

Bioassay-guided fractionation was performed using silica column chromatography to identify constituents of the *M. pyrifera* extract responsible for its anti-inflammatory effects. Forty fractions (F1-F40) were generated then evaluated in LTA-stimulated THP-1 cells, with fraction F25 showing the greatest inhibition of MCP-1 production (**Fig. 7S**, Supporting Information). F25 showed dose-dependent suppression of MCP-1 production that was significantly reduced from 0.25 mg.mL^{-1} relative to vehicle-treated cells ($p \leq 0.05$) (▶ **Fig. 4**). However, F25 caused a loss of viability in THP-1 cells at concentrations of 0.5 mg.mL^{-1} or greater ($p \leq 0.05$) (**Fig. 8S**, Supporting Information).

Bioactive compounds in the *M. pyrifera* extract and F25 were identified using RP-HPLC and GC-MS analyses, respectively. RP-HPLC revealed a peak for all-trans fucoxanthin in the extract that corresponded to 36.98 ± 2.35 ppm or 0.04 mg.mL^{-1}, while negligible peaks were present in F25 (**Fig. 9S**, Supporting Information). GC-MS analysis of the *M. pyrifera* extract and F25 identified saturated, monounsaturated, and polyunsaturated fatty acids (**Fig. 10S**, Supporting Information). Quantification of each fatty acid as a percentage of total (▶ **Table 1**) revealed saturated fatty acids were most abundant (extract: ≈ 37 %; F25: ≈ 52 %) with myristic acid as the major constituent (extract: ≈ 19 %, F25: ≈ 14 %). Oleic acid (extract: ≈ 17 %, F25: ≈ 14 %) and palmitoleic acid (extract: ≈ 1 %, F25: ≈ 1 %) were the most abundant monounsaturated fatty acids. Omega-6 and omega-3 polyunsaturated fatty acids were present in smaller proportions, with arachidonic acid being the most abundant omega-6 fatty acid (extract: ≈ 14 %, F25: ≈ 8 %), while stearidonic acid (extract: ≈ 10 %, F25: ≈ 9 %) and α-linolenic acid (extract: ≈ 10 %, F25: ≈ 8 %) were most abundant in omega-3 fatty acids found in the lipid extract and fraction.

Individual fatty acids abundant within the *M. pyrifera* extract and F25 were next assessed for their effect on MCP-1 production in LTA-stimulated THP-1 cells at equivalent concentrations as F25. Myristic acid, palmitoleic acid, and α-linolenic acid suppressed MCP-1 production relative to stimulated cells (≈ 69 %, ≈ 117 %, and ≈ 150 %, respectively, $p \leq 0.05$) (▶ **Fig. 5a**), without the cytotoxic effect observed for arachidonic acid ($p \leq 0.05$) (**Fig. 11Sa**, Supporting Information). Next, LTA-stimulated THP-1 cells were treated with a combination of the fatty acids. MCP-1 production was significantly reduced relative to stimulated THP-1 cells (neat ≈ 127 %, ½ dilution ≈ 93 %, $p \leq 0.05$) (▶ **Fig. 5b**), but only at concentrations that significantly reduced cell viability (neat: ≈ 53 %, ½ dilution: ≈ 17 %, $p \leq 0.05$) (**Fig. 11Sb**, Supporting Information).

Discussion

This study provides the first evidence of anti-inflammatory activity for a lipid extract from *M. pyrifera*. This extract reduced the expression of IL-1β and MCP-1 by THP-1 monocytes when applied 6 h prior, concurrently, or up to 6 h after stimulation with LTA. The extract also inhibited LPS-induced MCP-1 production by THP-1 monocytes. Lipid extracts from *P. palmata* and *I. okamurae* have been shown to suppress LPS-induced production of IL-8 and IL-1β in macrophages [16, 18]. Differences in the ability of these extracts to suppress specific proinflammatory mediators likely relate to variation in dosage, cell type, stimulation method, and treatment timing. This indicates care must be taken when developing treatment regimens utilizing seaweed-derived extracts. Importantly, the anti-inflammatory effects of the *M. pyrifera* extract for human monocytes were observed at a nontoxic concentration of 0.13 mg.mL^{-1}, which was consistent with the dosage applied for lipid extracts from other algae [18, 25]. A key aspect of this study was that it established a therapeutic window for using the *M. pyrifera* extract as an anti-inflammatory. Previous reports of anti-inflammatory algal-derived extracts and compounds were inconsistent in their study design, with treatments administered from 24 h to 30 min prior to the inflammatory stimuli [18, 20, 25, 26]. Here, the greatest extract activity was observed when applied 6 h prior, concurrently with, or up to 6 h after the inflammatory stimuli. This suggests the extract may be used prophylactically to reduce acute inflammation.

It is well established that TLR-induced NFκB signaling plays a critical role in the regulation of inflammation. The ethanolic extract of *Sargassum horneri* decreased phosphorylation of NFκB p50 and p65 subunits, while the sulphated polysaccharide isolated from *Sargassum swartzii* inhibited MyD88 production and TLR2/4 gene expression, as well as phosphorylation and translocation of NFκB p65, in LPS-activated macrophages [27, 28]. In our study, *M. pyrifera* extract reduced MYD88 and NFκB2/p100 protein levels and the phosphorylation of RelA/p65 in LTA-activated monocytes, which indicates the extract inhibits both canonical and non-canonical NFκB pathways [6, 7]. The canonical NFκB pathway is activated via both TLR2 and TLR4 [9, 10], so it is likely that extract inhibition of LTA- and LPS-induced proinflammatory cytokine and chemokine production is mediated via this pathway. However, the mechanism

▶ **Table 1** Fatty acid composition of *M. pyrifera* extract and fraction F25. Values are expressed as a percentage (%) of total FAMEs.

Lipid numbers	Retention time (min)	Common name	% Total FAMEs	
Saturated			**lipid extract**	**F25**
C12:0	6.50	Lauric acid	0.144	0.174
C13:0	7.11	Tridecanoic acid	0.281	0.262
C14:0	7.87	Myristic acid	18.649	14.160
Ci15:0	8.58	Pentadecylic acid	0.068	0.064
C16:0	9.95	Palmitic acid	0.147	21.230
C17:0	11.13	Margaric acid	0.142	0.142
C18:0	12.57	Stearic acid	1.761	1.642
C19:0	14.27	Nonadecylic acid	15.090	13.706
C20:0	16.21	Arachidic acid	0.454	0.330
Total			**36.736**	**51.71**
Monounsaturated				
C14:1	8.18	Myristic acid	0.145	0.140
C16:1	10.24	Palmitoleic acid	1.256	1.013
C18:1	13.17	Oleic acid	16.924	14.338
C22:1	21.29	Erucic acid	0.000	0.068
Total			**18.325**	**15.559**
Polyunsaturated				
Omega-6				
C18:3n-6	15.06	γ-linolenic acid	0.250	0.196
C20:4n-6	19.79	Arachidonic acid	13.542	8.435
C22:4	20.96		0.721	0.402
Total			**14.513**	**9.033**
Omega-3				
C18:3n-3	15.83	α-linolenic acid	9.940	7.956
C18:4n-3	16.67	Stearidonic acid	10.112	8.564
C22:3	19.14		0.373	0.173
C22:5n-3	21.65	Docosapentaenoic acid	10.001	7.005
Total			**30.426**	**23.698**

Concentration of *M. pyrifera* lipid extract and fraction 25 (F25): 1 mg.mL^{-1}.

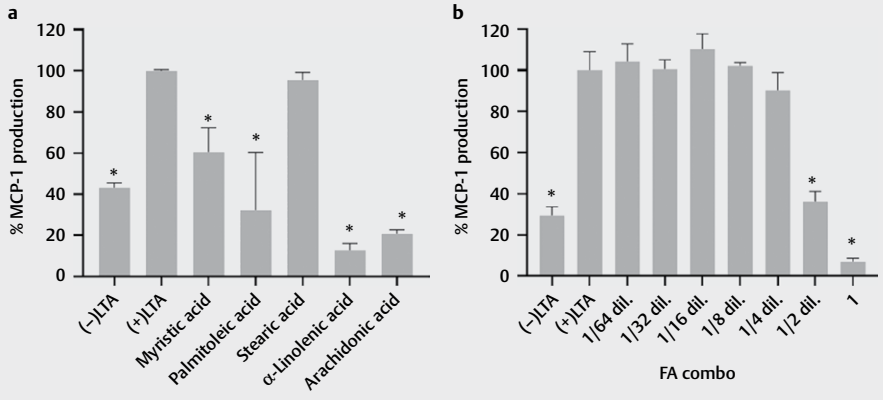

▶ **Fig. 5** Suppression of MCP-1 production in stimulated THP-1 cells by fatty acids identified within *M. pyrifera* fraction F25. THP-1 cells were stimulated by LTA (1 µg.mL^{-1}) with or without cotreatment with selected fatty acids at concentrations equivalent to that in F25, either (**a**) individually or (**b**) in combination with increasing dilution. After 24 h incubation, the conditioned medium was collected and assayed for MCP-1 production by ELISA. Values are expressed as percentage of the (+)LTA control and presented as the mean ± SD (n = 3), with those that differ significantly from (+) LTA control identified by one-way ANOVA followed by Dunnett's test ($^{*}p \leq 0.05$).

by which the extract modulates these signaling proteins is yet to be determined.

Our phytochemical analysis of the *M. pyrifera* extract provided insight into its anti-inflammatory constituents. The extract had a total lipid content of 1.5 % of the dry weight, consistent with previous results [23, 27, 28]. The 4 % fucoxanthin level was typical for other brown seaweeds [29]. This antioxidant has been shown to dampen inflammation by inhibiting NFκB activation and mitogen-activated protein kinase phosphorylation [19, 21]. However, the most potent *M. pyrifera* fraction lacked this pigment. Fatty acids found in the extract and fraction included saturated myristic and stearic acids, monounsaturated palmitoleic acid, and polyunsaturated α-linolenic and arachidonic acids. But only myristic, palmitoleic, and linolenic acids had anti-inflammatory effects, without exhibiting toxicity, when evaluated at quantities identified in the *M. pyrifera* fraction. Palmitoleic acid inhibited the expression of PPARα, an inhibitor of NFκB, in LPS-stimulated macrophages, and reduced MCP-1, IL-6, and IL-8 production in TNF-stimulated endothelial cells [30], Similarly, α-linolenic acid inhibited LPS-induced IL-1β, IL-6, and TNF-α production in THP-1 monocytes [31]. Myristic acid also reduced inflammation in a zebrafish model of *Candida* infection, showing synergy with palmitic acid [32].

The fatty acids identified within the *M. pyrifera* fraction, when combined, exhibited cytotoxicity without synergistic anti-inflammatory effects, likely due to the cytotoxicity observed for arachidonic acid. Arachidonic acid has been shown to induce macrophage cell cycle arrest through the stress-activated protein kinase pathway [33]. These findings suggest that the *M. pyrifera* extract contains other constituents that may provide cytoprotective properties that negate the cytotoxic effect of arachidonic acid. Monounsaturated fatty acids (palmitoleate and oleate) reduced toxicity in insulin-secreting cells [34], while fucoxanthin isolated from *S. siliquastrum* was cytoprotective against hydrogen peroxide-induced damage to fibroblasts [19], hepatic cells [35], and retinal pigment epithelial cells [36]. Further analyses are required to ascertain whether these effects extend to monocytes and in the presence of anti-inflammatory fatty acids.

Our study found that an extract, fraction, and specific fatty acids from *M. pyrifera* exert an anti-inflammatory effect on human monocytes stimulated through TLR2. These effects were mediated by signaling proteins and resulted in reduced proinflammatory cytokine and chemokine production at the mRNA and protein levels (▶ **Fig. 6**). This research has demonstrated the therapeutic potential of *M. pyrifera* lipids, while enhancing understanding as to their application and molecular targets. Further investigations are required to ascertain which constituents of the *M. pyrifera* extract may provide beneficial synergistic anti-inflammatory and cytoprotective effects and to define their mechanisms of action.

Materials and Methods

Solvent extraction

Fresh *M. pyrifera* samples were collected at Wellers Rock, Otago Harbour, New Zealand, in October 2018. The identification and authentication of plant material was carried out by Dr. Mike Stuart, a marine biologist affiliated with Te Rūnanga ō Ōtakou Marae, Dunedin, New Zealand and the voucher specimen was deposited in the University of Otago Herbarium, Dunedin, New Zealand (identifier: OTA72991). Samples were transported fresh, rinsed with H_2O, then dried at 25 °C for 48 h under circulating air, cut into small pieces, and stored in the dark at 4 °C. Seaweed pieces (20 g) were macerated in methanol:chloroform [EMSURE, analytical grade, 200 mL, 2:1 (v/v)]. Macerate was continuously swirled at 200 rpm at 36 °C for 2 h in the dark before filtering with Whatman filter paper no. 1. The filtrate was subjected to phase separation with 0.9 % NaCl (w/v) at a ratio of 2:1 (v/v) for 30 min in a separating funnel. The chloroform layer at the bottom of the flask was collected and evaporated using a vacuum rotary evaporator at 50–55 °C. The crude extract was stored at − 20 °C until further analysis. Three independent extractions were performed from the dried seaweed.

THP-1 cell culture and viability

Human monocytic leukemia THP-1 cell line was cultured in Roswell Park Memorial Institute 1640 medium (GIBCO Inc.) with 10 % heat-inactivated FBS (HyClone Laboratories), 2 mM sodium pyruvate (GIBCO Inc.), 50 U.mL^{-1} penicillin-streptomycin, and 60 µg.mL^{-1} kanamycin sulfate (Thermo Fisher Scientific).

THP-1 cells (1×10^5 cells.mL^{-1}) were incubated with absolute ethanol (EMSURE, analytical grade), extract, F25, or fatty acids solubilized in 1 % (v/v) ethanol at varying concentrations overnight in 5 % CO_2 at 37 °C. THP-1 cells were incubated with MTT (5 mg.mL^{-1}; Sigma) dissolved in PBS (Oxoid) overnight at 37 °C. Formazan crystals were solubilized with 10 % SDS buffer [(w/v) in 0.01 N HCl, pH 7.4], with incubation in the dark at 37 °C. Absorbance was read at 540 nm with the percentage of viable cells calculated relative to the vehicle only control (1 % ethanol).

THP-1 cell stimulation

THP-1 cells (1×10^6 cells.mL^{-1}) were stimulated with LTA (1 µg.mL^{-1}, *S. aureus* derived, purity > 97 %; Sigma) or LPS (1 µg.mL^{-1}, *Escherichia coli* 055:B5 derived, purity > 97 %; Sigma). Where indicated, cells were treated with the extract, F25, or fatty acids dissolved in 1 % ethanol (v/v) either 2, 6, or 24 h prior to (pretreatment), at the same time as (cotreatment), or 2, 6, or 24 h after (posttreatment) the addition of LTA or LPS. Recombinant human IL-10 (10 ng.mL^{-1}, *Escherichia coli* produced, purity > 98 %; Biolegend) was applied to cells concurrently with LTA or LPS stimulation. For cytokine analyses, the conditioned medium was collected by centrifugation after 24 h incubation with the stimulant and extract, then stored at − 80 °C. For mRNA analyses, the cells were collected by centrifugation after 0, 3, 4, 6, or 24 h incubation with the stimulant and extract, followed by mRNA extraction. For the proteome and Western blot analyses, cells (5×10^6 cells.mL^{-1}) were incubated for 4 h, followed by protein extraction using lysis buffer 6 (Proteome Profiler Array, R&D Systems) or sample buffer (0.5 M Tris-HCl pH 6.8, 2 % SDS, 10 % glycerol, 1 % β-mercaptoethanol, and 0.03 % bromophenol blue), then processed immediately. For immunocytochemistry, cells (2.5×10^6 cells.mL^{-1}) were seeded on a glass coverslip (8 mm diameter) and treated with 50 ng.mL^{-1} phorbol myristate acetate for 24 h at 37 °C prior to stimulation. After 4 h incubation with stimuli and treatment, cells were fixed with ice cold methanol, then processed immediately.

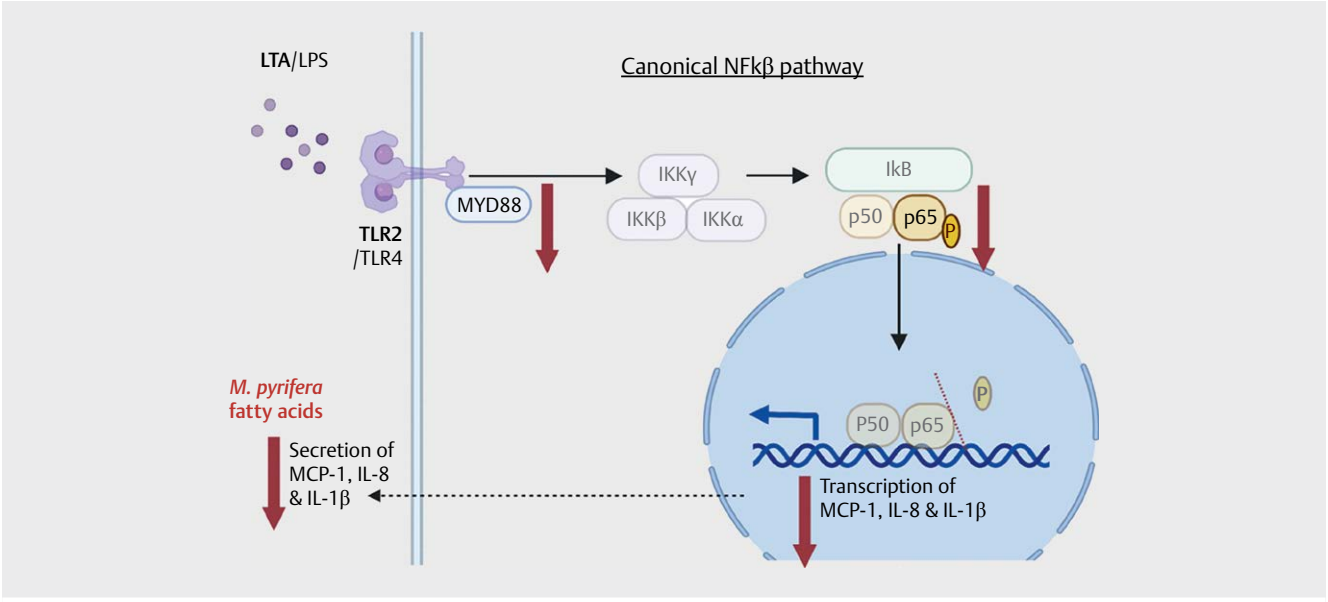

▶ **Fig. 6** Schematic representation of the anti-inflammatory effects of *M. pyrifera* extract on TLR2-mediated NFκB signaling in human monocytes. This fatty acid-rich extract reduced MCP-1, IL-8, and IL-1β secretion from LTA-stimulated THP-1 monocytes through suppression of canonical NFκB signaling, with decreased MYD88 abundance, RelA/p65 phosphorylation, and gene transcription. The extract also reduced MCP-1 secretion following TLR4 activation via LPS. Red arrows depict steps within the canonical NFκB pathway, shown in this study to be suppressed by the *M. pyrifera* extract. Created with BioRender.com

Cytokine ELISAs

Cytokine and chemokine levels within the cell conditioned medium were quantified using BD-OptEI ELISA kits (MCP-1, #555179; IL-8, #555244; IL-1β, #557953) in accordance with the manufacturer's instructions. Protein production normalized to LTA-stimulated cells at an equivalent timepoint.

Quantitative PCR

Total RNA was isolated using a GENEzol TriRNA Pure Kit (Geneaid Biotech Ltd.). First strand cDNA was generated using a qScript cDNA Synthesis Kit (QuantaBio). Quantitative PCR was conducted using the cDNA equivalent of 5 ng RNA, 200 mM of each primer, and Fast SYBR Green Master Mix (Thermo Fisher Scientific) on the Mic qPCR Cycler (Bio Molecular Systems). The primer pairs and their efficiencies are listed in **Table 1S**, Supporting Information. Gene expression was normalized to GAPDH and LTA-stimulated cells.

NF-κB proteome analysis

A Proteome Profiler Human NF-κB Pathway Array kit was used and analyses were performed as instructed (R&D Systems). Lysates were incubated with membranes overnight, followed by incubation with biotin-conjugated anti-cytokine antibodies for 1 h and HRP-conjugated streptavidin for 30 min. The chemiluminescent signals were detected on CL-XPosure films (Thermo Fisher Scientific). For each membrane, the image threshold was adjusted, and spot density was quantified using ImageJ (https://imagej.nih.gov/ij), with normalization to reference spots and LTA-stimulated cells.

Western blot analysis

Rabbit anti-MYD88 (ab2064; 1:1000), anti-β-tubulin (ab6046; 1:10000), and goat anti-rabbit IgG (H&L)-HRP (ab6721; 1:3000) antibodies were purchased from Abcam. Lysates were boiled then separated by SDS-PAGE using a 12 % gel. Proteins were transferred onto a nitrocellulose membrane (0.45 µm; Bio-Rad Laboratories), then blocked with 5 % (w/v) nonfat milk in Tris-buffered saline (50 mM Tris, pH 7.6, 150 mM NaCl, and 1 % (v/v) Tween 20) for 1 h at room temperature. Membranes were incubated with primary antibodies in PBS [with 0.05 % (v/v) Tween 20] overnight at 4 °C, secondary antibody for 1 h at room temperature, then SuperSignal West Pico PLUS substrate (Thermo Fisher Scientific) for 5 min. Signals were visualized using an Uvitec Alliance gel imaging system. Band densities were quantified using Image J, then normalized to loading control (β-tubulin) and LTA-stimulated cells.

Immunocytochemistry

Rabbit anti-MYD88 (ab2064; 1:100) was used with AlexaFluor-594-goat anti-rabbit IgG (H + L) (A-11072; 1:500) and DAPI (1:1000), purchased from Invitrogen. Fixed cells were permeabilized with 0.1 % Triton X-100 and 0.05 % Tween 20 (v/v) in PBS for 10 min, then blocked with 1 % bovine serum albumin (w/v) and 0.1 % Tween 20 in 300 mM glycine for 30 min. Cells were incubated with primary antibody overnight at 4 °C, secondary antibody for 1 h at room temperature, and by 30 min with DAPI at room temperature in the dark. Coverslips were mounted on glass slides with SlowFade gold antifade reagent (Invitrogen).

Images were captured on an Eclipse No-E upright fluorescence microscope and NIS-Elements D Software for DAPI (excitation 358 nm; emission 461 nm) and Alexa Fluor-594 (excitation 590 nm; emission 617 nm). The average fluorescence intensity was performed on five high power fields (×40 objective) per stain and coverslip using ImageJ, following RGB channel split and threshold adjustment, with normalization to DAPI and LTA-stimulated cells.

Silica column fractionation

A glass column with grit (250 mm × 15 mm) was packed with a slurry of silica gel 60 [8 g in 40 mL hexane (70–230 mesh; Merck)]. The extract (10 mg) was dissolved in chloroform, loaded into the column, then eluted with chloroform (20 mL), methanol:chloroform (1:1, 20 mL), and methanol (40 mL) in order of increasing polarity. Forty fractions (F1-F40, ≈ 1 mL each) were collected then dried in the fume hood overnight at room temperature, with storage at −20 °C.

GC-MS

FAMEs were analyzed using a Thermo-Fisher TRACE 1300 GC equipped with an ISQ 7000 single quadrupole MS equipped with a Restek Rxi-5Sil MS column. Parameters for analysis of FAMEs are shown in **Table 2S**, Supporting Information. Obtained mass spectra were further evaluated employing the NIST database (MS Search; NIST, MSS Ltd.). The proportion of each fatty acid is reported as percentage of total integrated fatty acid peak areas for each chromatogram.

RP-HPLC

RP-HPLC analyses were carried out using a Shimadzu Prominence HPLC system equipped with a pump (LC-20AD), an autosampler (SIL-20A), and a photo-diode array spectrophotometric detector (SPD-M20). The parameters for analysis of fucoxanthin are shown in **Table 3S**, Supporting Information). All-trans-fucoxanthin (#F6932, purity ≥ 95 %; Sigma) was used as a reference to determine the retention time (7.23 min) and for preparation of a standard curve (area vs. concentration). Fucoxanthin content in the extract (1 $mg.mL^{-1}$) and fraction (4 $mg.mL^{-1}$) was quantified using the standard curve and expressed as parts per million (ppm).

Preparation of commercial fatty acids

Myristic acid (#M3128, purity ≥ 99 %), palmitic acid (#P0500, purity ≥ 99 %), stearic acid (#175366, purity = 95 %), palmitoleic acid (#P9417, purity ≥ 98.5 %), arachidonic acid (# A3611, purity ≥ 98.5 %), and linolenic acid (#L2376, purity ≥ 99 %) were purchased from Sigma. Individual and combination fatty acid solutions were prepared in 1 % ethanol, then for cell treatments, were diluted in RPMI to concentrations equivalent to that in F25: myristic acid, 0.622 µM; palmitic acid, 0.827 µM; stearic acid, 0.058 µM; palmitoleic acid, 0.040 µM; α- linolenic acid, 0.277 µM; and arachidonic acid, 0.286 µM.

Statistical analysis

Values are expressed as the mean ± SD. For the biological analyses, a single *M. pyrifera* extract and F25 fraction were assessed in at least three independent experiments. A Shapiro-Wilk normality test was performed to confirm normal distribution of the data, followed by one-way analysis of variance (ANOVA) and a Dunnett's test to determine significant points of difference between means. Values of $p \leq 0.05$ were considered statistically significant.

Acknowledgments

Dr. Mike Stuart (Te Rūnanga ō Ōtakou Marae) for assisting in the collection and identification of the seaweed samples, Dr. Daniel Killeen (The New Zealand Institute for Plant & Food Research Limited) for assistance with GC-MS analyses, Kevin Crump (Department of Pharmacy) for assistance with RP-HPLC analyses, and Gabriella Stuart (Department of Pharmacology and Toxicology) for training in quantitative PCR.

Conflict of Interest

The authors declare that they have no conflict of interest.

References

[1] Hernandez-Carmona G, Rodriguez E, Casas M, Sánchez I. Evaluation of the beds of Macrocystis pyrifera (Phaeophyta, Laminariales) in the Baja California Peninsula, Mexico. III. Summer 1986 and seasonal variation. Cienc Mar 1991; 17: 121–145

[2] Buschmann AH, Camus C, Infante J, Neori A, Israel Á, Hernández-González MC, Pereda SV, Gomez-Pinchetti JL, Golberg A, Tadmor-Shalev N. Seaweed production: overview of the global state of exploitation, farming and emerging research activity. Eur J Phycol 2017; 52: 391–406

[3] Purcell-Meyerink D, Packer MA, Wheeler TT, Hayes M. Aquaculture Production of the Brown Seaweeds Laminaria digitata and Macrocystis pyrifera: Applications in Food and Pharmaceuticals. Molecules 2021; 26: 1306

[4] Fernando IP, Kim M, Son KT, Jeong Y, Jeon YJ. Antioxidant Activity of Marine Algal Polyphenolic Compounds: A Mechanistic Approach. J Med Food 2016; 19: 615–628

[5] Netea MG, Balkwill F, Chonchol M, Cominelli F, Donath MY, Giamarellos-Bourboulis EJ, Golenbock D, Gresnigt MS, Heneka MT, Hoffman HM, Hotchkiss R, Joosten LAB, Kastner DL, Korte M, Latx E, Libby P, Mandrup-Poulsen T, Mantovani A, Mills KHG, Nowak KL, O'Neill LA, Pickkers P, van der Poll T, Ridker PM, Schalkwijk J, Schwartz DA, Siegmund B, Steer CJ, Tilg H, van der Meer JWM, van der Veerdonk FL, Dinarell CA. A guiding map for inflammation. Nat Immunol 2017; 18: 826–831

[6] Kawai T, Akira S. Signaling to NF-κB by Toll-like receptors. Trends Mol Med 2007; 13: 460–469

[7] Mogensen TH. Pathogen recognition and inflammatory signaling in innate immune defenses. Clin Microbiol Rev 2009; 22: 240–273

[8] Takeuchi O, Hoshino K, Kawai T, Sanjo H, Takada H, Ogawa T, Takeda K, Akira S. Differential roles of TLR2 and TLR4 in recognition of gram-negative and gram-positive bacterial cell wall components. Immunity 1999; 11: 443–451

[9] Munford RS. Sensing gram-negative bacterial lipopolysaccharides: a human disease determinant? Infect Immun 2008; 76: 454–465

[10] Fournier B. The function of TLR2 during staphylococcal diseases. Front Cell Infect Microbiol 2013; 2: 167, 1–8

[11] Aliprantis AO, Yang RB, Weiss DS, Godowski P, Zychlinsky A. The apoptotic signaling pathway activated by Toll-like receptor-2. EMBO J 2000; 19: 3325–3336

[12] Lee J, Banu SK, Subbarao T, Starzinski-Powitz A, Arosh JA. Selective inhibition of prostaglandin E2 receptors EP2 and EP4 inhibits invasion of human immortalized endometriotic epithelial and stromal cells through suppression of metalloproteinases. Mol Cell Endocrinol 2011; 332: 306–313

[13] Sostres C, Gargallo CJ, Arroyo MT, Lanas A. Adverse effects of non-steroidal anti-inflammatory drugs (NSAIDs, aspirin and coxibs) on upper gastrointestinal tract. Best Pract Res Clin Gastroentero 2010; 24: 121–132

[14] Hörl WH. Nonsteroidal anti-inflammatory drugs and the kidney. Pharmaceuticals 2010; 3: 2291–2321

[15] Wöhrl S. NSAID hypersensitivity – recommendations for diagnostic work up and patient management. Allgro J Int 2018; 27: 114–121

[16] Robertson RC, Guihéneuf F, Bahar B, Schmid M, Stengel DB, Fitzgerald GF, Ross RP, Stanton C. The anti-inflammatory effect of algae-derived lipid extracts on lipopolysaccharide (LPS)-stimulated human THP-1 macrophages. Mar Drugs 2015; 13: 5402–5424

[17] Kim MM, Rajapakse N, Kim SK. Anti-inflammatory effect of Ishige okamurae ethanolic extract via inhibition of NF-kappaB transcription factor in RAW 264.7 cells. Phytother Res 2009; 23: 628–634

[18] Heo SJ, Ko SC, Kang SM, Kang HS, Kim JP, Kim SH, Lee KW, Cho MG, Jeon YJ. Cytoprotective effect of fucoxanthin isolated from brown algae Sargassum siliquastrum against H2O2-induced cell damage. Eur Food Res Technol 2008; 228: 145–151

[19] Heo SJ, Yoon WJ, Kim KN, Ahn GN, Kang SM, Kang DH, Affan A, Oh C, Jung WK, Jeon YJ. Evaluation of anti-inflammatory effect of fucoxanthin isolated from brown algae in lipopolysaccharide-stimulated RAW 264.7 macrophages. Food Chem Toxicol 2010; 48: 2045–2051

[20] Kim KN, Heo SJ, Yoon WJ, Kang SM, Ahn G, Yi TH, Jeon YJ. Fucoxanthin inhibits the inflammatory response by suppressing the activation of NF-κB and MAPKs in lipopolysaccharide-induced RAW 264.7 macrophages. Eur J Pharmacol 2010; 649: 369–375

[21] Zhang W, Oda T, Yu Q, Jin JO. Fucoidan from Macrocystis pyrifera has powerful immune-modulatory effects compared to three other fucoidans. Mar Drugs 2015; 13: 1084–1104

[22] Ortiz J, Uquiche E, Robert P, Romero N, Quitral V, Llantén C. Functional and nutritional value of the Chilean seaweeds Codium fragile, Gracilaria chilensis and Macrocystis pyrifera. Eur J Lipid Sci Technol 2009; 111: 320–327

[23] Nguyen S, Nguyen H, Truong K. Comparative cytotoxic effects of methanol, ethanol and DMSO on human cancer cell lines. Biomed Res Ther 2020; 7: 3855–3859

[24] Iyer SS, Cheng G. Role of interleukin 10 transcriptional regulation in inflammation and autoimmune disease. Crit Rev Immunol 2012; 32: 23–63

[25] Gil TY, Kang YM, Eom YJ, Hong CH, An HJ. Anti-Atopic Dermatitis Effect of Seaweed Fulvescens Extract via Inhibiting the STAT1 Pathway. Mediators Inflamm 2019; 2019: 3760934

[26] Khan MN, Cho JY, Lee MC, Kang JY, Park NG, Fujii H, Hong YK. Isolation of two anti-inflammatory and one pro-inflammatory polyunsaturated fatty acids from the brown seaweed Undaria pinnatifida. J Agric Food Chem 2007; 55: 6984–6988

[27] Jayawardena TU, Kim HS, Sanjeewa KA, Kim SY, Rho JR, Jee Y, Ahn G, Jeon YJ. Sargassum horneri and isolated 6-hydroxy-4, 4, 7a-trimethyl-5, 6, 7, 7a-tetrahydrobenzofuran-2 (4H)-one (HTT); LPS-induced inflammation attenuation via suppressing NF-κB, MAPK and oxidative stress through Nrf2/HO-1 pathways in RAW 264.7 macrophages. Algal Res 2019; 40: 101513

[28] Jayawardena TU, Sanjeewa K, Nagahawatta D, Lee HG, Lu YA, Vaas A, Abeytunga DTU, Nanayakkara CM, Lee DS, Jeon YJ. Anti-Inflammatory Effects of Sulfated Polysaccharide from Sargassum Swartzii in Macrophages via Blocking TLR/NF-Kβ Signal Transduction. Mar Drugs 2020; 18: 601

[29] Xia S, Wang K, Wan L, Li A, Hu Q, Zhang C. Production, characterization, and antioxidant activity of fucoxanthin from the marine diatom Odontella aurita. Mar Drugs 2013; 11: 2667–2681

[30] Souza CO, Teixeira AA, Biondo LA, Silveira LS, Calder PC, Rosa Neto JC. Palmitoleic acid reduces the inflammation in LPS-stimulated macrophages by inhibition of NFκB, independently of PPARs. Clin Exp Pharmacol Physiol 2017; 44: 566–575

[31] Pauls SD, Rodway LA, Winter T, Taylor CG, Zahradka P, Aukema HM. Anti-inflammatory effects of α-linolenic acid in M1-like macrophages are associated with enhanced production of oxylipins from α-linolenic and linoleic acid. J Nutr Biochem 2018; 57: 121–129

[32] Prasath KG, Alexpandi R, Parasuraman R, Pavithra M, Ravi AV, Pandian SK. Anti-inflammatory potential of myristic acid and palmitic acid synergism against systemic candidiasis in Danio rerio (Zebrafish). Biomed Pharmacother 2021; 133: 111043

[33] Shen Z, Ma Y, Ji Z, Hao Y, Yan X, Zhong Y, Tan X, Ren W. Arachidonic acid induces macrophage cell cycle arrest through the JNK signaling pathway. Lipids Health Dis 2018; 17: 26, 1–9

[34] Diakogiannaki E, Dhayal S, Childs CE, Calder PC, Welters HJ, Morgan NG. Mechanisms involved in the cytotoxic and cytoprotective actions of saturated versus monounsaturated long-chain fatty acids in pancreatic β-cells. J Endocrinol 2007; 194: 283–291

[35] Wang X, Cui YJ, Qi J, Zhu MM, Zhang TL, Cheng M, Liu SM, Wang GC. Fucoxanthin Exerts Cytoprotective Effects against Hydrogen Peroxide-Induced Oxidative Damage in L02 Cells. Biomed Res Int 2018; 2018: 1085073

[36] Chen SJ, Lin TB, Peng HY, Liu HJ, Lee AS, Lin CH, Tseng KW. Cytoprotective potential of fucoxanthin in oxidative stress-induced age-related macular degeneration and retinal pigment epithelial cell senescence in vivo and in vitro. Mar Drugs 2021; 19: 114, 1–15